

Research Article

Artificial Membrane Induced by Novel Biodegradable Nanofibers in the Masquelet Procedure for Treatment of Segmental Bone Defects

Yi-Hsun Yu,^{1,2} Ren-Chin Wu,³ Demei Lee,³ Che-Kang Chen,³ and Shih-Jung Liu ^{2,4}

¹Department of Orthopedic Surgery, Musculoskeletal Research Center, Chang Gung Memorial Hospital-Linkou, Taoyuan, Taiwan

²Department of Mechanical Engineering, Chang Gung University, Taoyuan, Taiwan

³Department of Pathology, Chang Gung Memorial Hospital-Linkou, Tao-Yuan, Taiwan

⁴Department of Orthopedic Surgery, Chang Gung Memorial Hospital-Linkou, Taoyuan, Taiwan

Correspondence should be addressed to Shih-Jung Liu; shihjung@mail.cgu.edu.tw

Received 18 July 2018; Revised 22 August 2018; Accepted 6 September 2018; Published 23 October 2018

Guest Editor: Laura Tamayo

Copyright © 2018 Yi-Hsun Yu et al. This is an open access article distributed under the Creative Commons Attribution License, which permits unrestricted use, distribution, and reproduction in any medium, provided the original work is properly cited.

The Masquelet induced-membrane technique for the treatment of segmental bone defects includes a two-stage surgical procedure, and polymethylmethacrylate (PMMA) plays a major role in the treatment. However, the PMMA spacer must be surgically removed. Here, we investigated the potential of poly(lactic-co-glycolic acid) (PLGA) nanofibers, a biodegradable material to replace the PMMA spacer, allowing the bioactive membrane to be induced and the spacer to degrade without the additional surgery on a rabbit femoral segmental bone defect model. PLGA nanofibers were shown to degrade completely six weeks after implantation in the investigated animals, and a thick membrane was found to circumferentially fold around the segmental bone defects. Results from image studies demonstrated that, in the group without the bone graft, all studied femurs exhibited either nonunion or considerable malunion. In contrast, the femurs in the bone graft group had a high union rate without considerable deformities. Histological examinations suggested that the membranous tissue in this group was rich in small blood vessels and the expression of BMP2 and VEGF increased. Our results demonstrate that the biodegradable PLGA nanofibers may be useful for replacing the PMMA spacer as the bioactive-membrane inducer, facilitating the process of healing and removing the need for repeated surgeries.

1. Introduction

Segmental bone defects may be a result of trauma, tumor resection, or the sequelae of osteomyelitis, and their management remains challenging for orthopedic surgeons [1, 2]. Additionally, the development of these defects is accompanied by considerable functional disabilities in patients. Two approaches have been commonly employed for the treatment of segmental bone defects. First, the transplantation of vascularized autologous bone graft [2–4] has been commonly used; however, the donor site morbidity from the autologous fibula graft, including infection and stress fracture, remains as the main concern. In addition, the operation must be performed by a microsurgery specialist [4]. The second approach is the bone transport with distraction osteogenesis by the Ilizarov

ring fixator, which is a standard procedure for the management of segmental bone defect applied by experienced surgeons in some medical institutes [5–7]. Nevertheless, various complications, including pin tract infection, failure of the transported bone consolidation, and nonunion at the docking site, have been reported [8, 9].

An alternative approach for the segmental bone defect repair was first proposed by Masquelet et al. in 1980 [10], showing that, following the implantation of a polymethylmethacrylate (PMMA) spacer for 6 to 8 weeks in the segmental cortical bone defect, a periosteum-like membrane surrounding the defect, containing osteogenic and osteoinductive factors, can be induced. This PMMA-induced bioactive membrane serves as an envelope, encapsulating the autologous cancellous bone graft and promoting bone healing. Other

studies, following this two-stage Masquelet procedure, demonstrated satisfactory results for bone union [11–17]. In spite of the promising outcomes achieved using this technique, one major drawback pertains to the requirement for the surgical removal of the PMMA spacer, demanding the patients to undergo several surgeries, thus increasing the cost and complexity of the treatment.

Since the actual mechanisms underlying the formation of the induced membrane have not been completely elucidated, we aimed to examine whether the PMMA spacer can be replaced by a different biodegradable implant, in order to avoid the requirement for an additional surgical intervention during the Masquelet procedure. Therefore, we developed biodegradable nanofibrous implants and examined their ability to induce bioactive membranes using the segmental bone defect model. Additionally, we investigated the role of biodegradable implants as the reservoirs for bone grafting during the formation of the bioactive membrane, which facilitates fracture healing.

2. Materials and Methods

2.1. Preparation of Poly(Lactic-Co-Glycolic Acid) (PLGA) Nanofibers. PLGA polymers (LA:GA = 50:50, Sigma, USA) were adopted. An electrospinning setup was employed to produce the nanofibers. A high voltage of 17 kV was applied to the needle that emits the solution jet. The distance of the needle to the collecting plate and the flow rate of the syringe were 12 cm and 0.5 mL/h, respectively. A fabricated nanofibrous membrane was incubated in a chamber equipped with a vacuum pump at 40°C for three days to volatilize the solvent.

2.2. Scanning Electron Microscope (SEM) Characterization. The morphological structure of the polymeric fibers was characterized by a JEOL Model JSM-7500F field emission SEM (Tokyo, Japan).

2.3. In Vivo Study and Animal Care. This study and all procedures used acquired approval from the Institutional Review Board and Animal Care Center of Chang Gung University, Taiwan (IRB number: CGU106-058). Twelve 6-month-old male New Zealand rabbits were cared and grown using the standardized procedures of the Animal Care Center of Chang Gung University. The rabbits were housed in individual pens with free access to food and water. All the studied rabbits had comparable weights (3.0 ± 0.2 kg).

Prior to the surgeries, oxygen was delivered to the animals via a face mask at a flow rate of 4 L/min for five minutes. Isoflurane was then transmitted via the face mask till the rabbit became anesthetized and continued during the entire surgical procedure. Rabbits were kept in the decubitus position which allowed the surgical field upwards, and the right thighs were shaved and disinfected. A longitudinal incision was made along the lateral aspect of the thigh, and an internervous plane was created bluntly between the vastus lateralis and biceps femoris to expose the anterolateral aspect of the femur (Figure 1(a)). Afterward, the femur was fixed with a 10-hole stainless-steel plate (Lisen Technology Co. Ltd., New Taipei City, Taiwan) with two 2.0 mm screws

at each end, and a 1.8 mm Kirschner wire was inserted intramedullary from the intercondylar notch of the femur retrogradely. After stabilization, a critical-size bone defect, measuring 10 mm, was created in the middle of femur shaft using an osteotome (Figure 1(b)).

Following the creation of the defect, the defect was wrapped circumferentially with the PLGA nanofibers (Figure 1(c)), and we randomized the operated rabbits into two groups: bone graft-free (BG-f) and bone graft (BG) groups. In the BG-f group, the nanofibers were sutured at both ends with 3-0 Vicryl (Ethicon, Johnson & Johnson, New Jersey, USA) suture to secure the wrapping, leaving the inside of the wrapped nanofiber empty (Figure 1(d)), while in the BG group, the same wrapping procedure was completed after placing the bone chips, obtained from the osteotomized femur by chipping of the cortical bone, inside the wrapped PLGA nanofibers (Figure 1(e)).

Afterward, the wound was irrigated with sterile saline and the fascia of the vastus lateralis and biceps femoris were approximated using 2-0 Vicryl suture, while the subcutaneous tissue and skin were occluded using 3-0 Vicryl suture (Ethicon, Johnson & Johnson, New Jersey, USA).

All animals were monitored daily for any altered behavior or complications, and analgesics were administered for 5 days postoperatively. They were allowed free movements and full weight bearing immediately following the recovery from anesthesia. The rabbits were also checked twice daily for mentation and attitude, ability to ambulate, willingness to bear weight on the surgically treated limb, food and water consumption, respiratory rate, and inflammation at the surgical site.

All the rabbits were euthanized 6 weeks after the surgical procedure by a standard euthanasia procedure. The entire femur was harvested through the plane used in the previous surgical procedures. Periosteal and fibrous tissues surrounding the defects were preserved. The observed membranes were excised carefully and further analyzed. Femur samples were fixed in 10% neutral buffered formalin for 48 h and transferred to 70% ethanol, until further X-ray and micro-computed tomography (CT) studies.

2.4. X-Ray and Micro-CT Examinations. The animals underwent X-ray examinations twice: immediately after the surgical procedure and after euthanasia at six weeks. Prior to the first radiative inspection, the animals were consoled with an intravenous injection of zolazepam/tiletamine (Zoletil, Taipei, Taiwan). X-ray images of the anteroposterior and lateral views were obtained. During the second X-ray imaging, the target femora were evaluated using micro-CT as well.

2.5. Histologic Analysis

2.5.1. Capsular Tissue Processing. Capsular tissue samples obtained from the investigated animals were preserved in 10% phosphate-buffered formalin and sliced into 2 mm wide fragments, which were processed and embedded in paraffin. Tissue sections ($4 \mu\text{m}$) were obtained using a microtome (Sakura Finetek, Tokyo, Japan) for histological

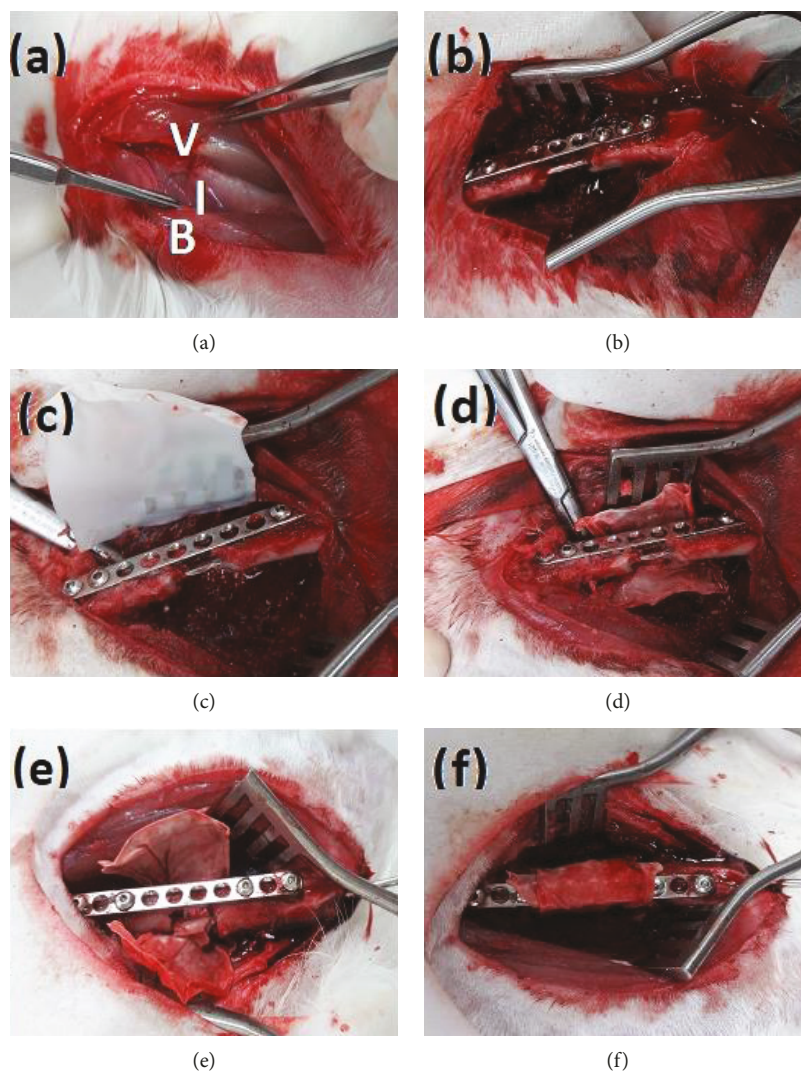


FIGURE 1: Surgical procedure applied for the formation and treatment of the segmental bone defect in a rabbit model. (a) Identification the internervous plane (I) between the vastus lateralis (V) and biceps femoris (B). (b) Creation of a 10 mm femoral defect following the fixation procedure with stainless plate and intramedullary nail. (c) Application of PLGA nanofibers around the bone defect. (d) Suture fixation of the PLGA nanofibers in the BG-f group. (e) Bone grafting (BG) inside the femoral defect before the suture-fixation of the PLGA nanofibers.

and immunohistochemical (IHC) evaluations. Additionally, the obtained samples were blotted with H&E and observed under a microscope with magnification up to 400x.

2.5.2. IHC Staining of Capsular Tissue. IHC staining was performed on $4\mu\text{m}$ tissue sections using an automated stainer (BOND-MAX, Leica Microsystems, Singapore). After deparaffinization, heat-induced epitope retrieval was performed ($100^{\circ}\text{C}/20\text{min}$) in EDTA buffer (pH9). For bone morphogenic protein (BMP2) analysis, a mouse anti-BMP2 monoclonal antibody (1:200; clone 65529.111, Cat# ab6285, Abcam, Cambridge, UK) was adopted as the primary antibody. For the characterization of the vascular endothelial growth factor (VEGF), a mouse anti-VEGF antibody (1:400; clone VG1, Cat#: NB100-664, Novus Biologicals, Littleton, CO, USA) was used. PolyTek goat anti-mouse polymerized horseradish peroxidase (HRP;

Scytek Laboratories, Logan, UT, USA) was employed as the secondary antibody. Bond Polymer Refine Detection Kit (DS9800, Leica Microsystems, Singapore) was applied for the visualization of obtained signals.

3. Results

3.1. SEM Analysis PLGA of Nanofibers. The microscopic photos of the biodegradable nanofibers are displayed in Figure 2 ($\times 8000$). Measured diameters of PLGA nanofibers spanned from 40 to 430 nm.

3.2. Femoral Sample Examination. After euthanizing the rabbits and excising the target femora, we observed that in all specimens, a membranous layer was observed to surround the applied PLGA nanofibers densely, immediately between the applied material and the muscles (Figure 3).

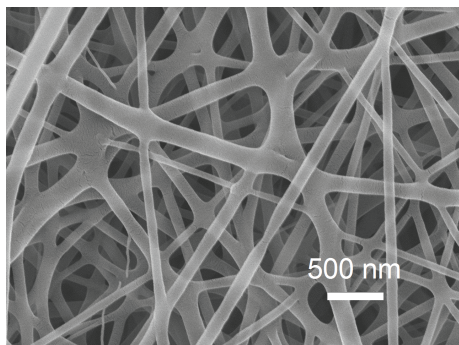


FIGURE 2: SEM photograph of the fabricated nanofibers.

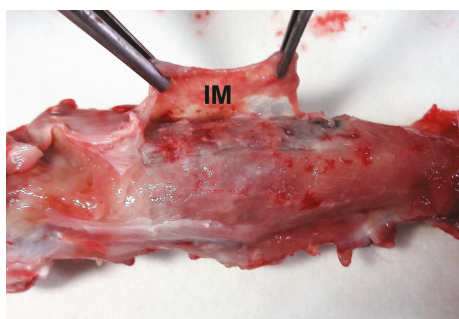


FIGURE 3: Induced-membrane formation. Identification of the induced membrane (IM) around the poly(lactic-co-glycolic acid) nanofibers in a representative rabbit femoral specimen.

In the BG group, the femoral samples were shown to have continuous hard calluses without any considerable deformities, shortening of the osteotomized femurs, or loosened implants (Figure 4(a)). In contrast, in the BG-f group, various adverse effects of the implantation were observed, such as residual fracture gap in the calluses, loosened screws, changes in the position of the intramedullary K wires, and considerable malunion rate and shortening of the femur (Figure 4(b)).

3.3. X-Ray and Micro-CT Results. As observed in the follow-up series of X-ray images obtained in the BG-f group, four femurs failed to achieve bone union, leading to the residual bony gaps, while two femurs were malunited with considerable deformity and shortening rates (Figure 5(a)). In contrast, in the BG group, only one femoral sample was shown to have a residual gap on one side. Five tissue samples were found to achieve bone union without serious deformities (Figure 5(b)), while one sample had a loosened implant with some degree of shortening and malunion. Micro-CT examinations revealed united bone gaps and good bone remodeling in the BG group (Figure 5(c)), with good callus formation and continuous femoral cortex.

3.4. Histologic and IHC Characteristics of the Capsules. The surfaces of the capsular membranes in both groups were found to be lined by one to three layers of round to ovoid cells or short spindle cells (Figure 6(a)). These cells were shown to

lack the underlying basement membrane and morphologically resembled synoviocytes. The deeper layers of the membranes consisted of fibroblast-like spindle cells with longer cytoplasmic processes and haphazard orientation in an extracellular matrix-rich stroma. Membranous tissue was rich in small blood vessels. Scattered eosinophils and lymphocytes were noted in most cases, and multinucleated giant cells were occasionally identified.

IHC staining revealed that the membrane-lining cells and spindle cells showed a diffuse and strong cytoplasmic expression of BMP2 (Figure 6(b)), with the moderate expression of VEGF, whereas the vascular endothelial cells exhibited intense cytoplasmic VEGF staining (Figure 6(c)).

4. Discussion

In this study, we examined the effectiveness of the PLGA nanofibers used in the Masquelet technique for the induction of a periosteum-like bioactive membrane and the repair of the segmental bone defects. Our results demonstrated that the bioactive membrane can be successfully induced by the application of the biodegradable material tested here, PLGA, which was shown to be accompanied by the expression of growth factors such as BMP2 and VEGF. PLGA nanofibers were shown to play an important role as the bone graft reservoirs, assisting fracture union in the segmental femoral defect model.

Biodegradable materials have been widely employed in medical procedures since the 1970s. They have been applied in orthopedic surgeries, as internal fixators [18, 19], drug delivery media [20–22], and bone graft reservoirs [23, 24]. PLGA has been one of the most prospective biodegradable polymers, mainly due to its controllable degradation and superior biocompatibility with human tissues. This polymeric material has received approval for clinical applications, owing to that it is innocuous, evokes an acceptable inflammation, and can be degraded via the hydrolysis of its ester bond [25]. These end products may induce inflammatory responses in the surrounding tissue, recruiting fibroblasts and inflammatory cells and stimulating angiogenesis. Additionally, we supposed that inflammatory responses due to the degradation of the biodegradable materials may induce tissue adhesion, leading to the formation of an encapsulated cavity, which may play a role as a reservoir for bone grafts. We demonstrated here that the PLGA fibers induced the formation of a mature periosteum-like membrane circumferentially wrapped around the fibers. These nanofibers were shown to be hydrolyzed and degraded at the time of examination, while the cells localized in the healing tissue expressed osteoinductive factors such as BMP2 and VEGF.

The Masquelet technique combined with a two-stage external and internal fixation has been widely accepted as a standard in the treatment of large bone defects: the first stage consists of radical debridement, limb stabilization, PMMA spacer implantation, and soft tissue coverage, while the second stage consists of the clearance of infection, if infective nonunion locations exist, removal of the PMMA spacer, massive autologous cancellous bone grafting, and a permanent internal fixation [26–28]. The implantation of the

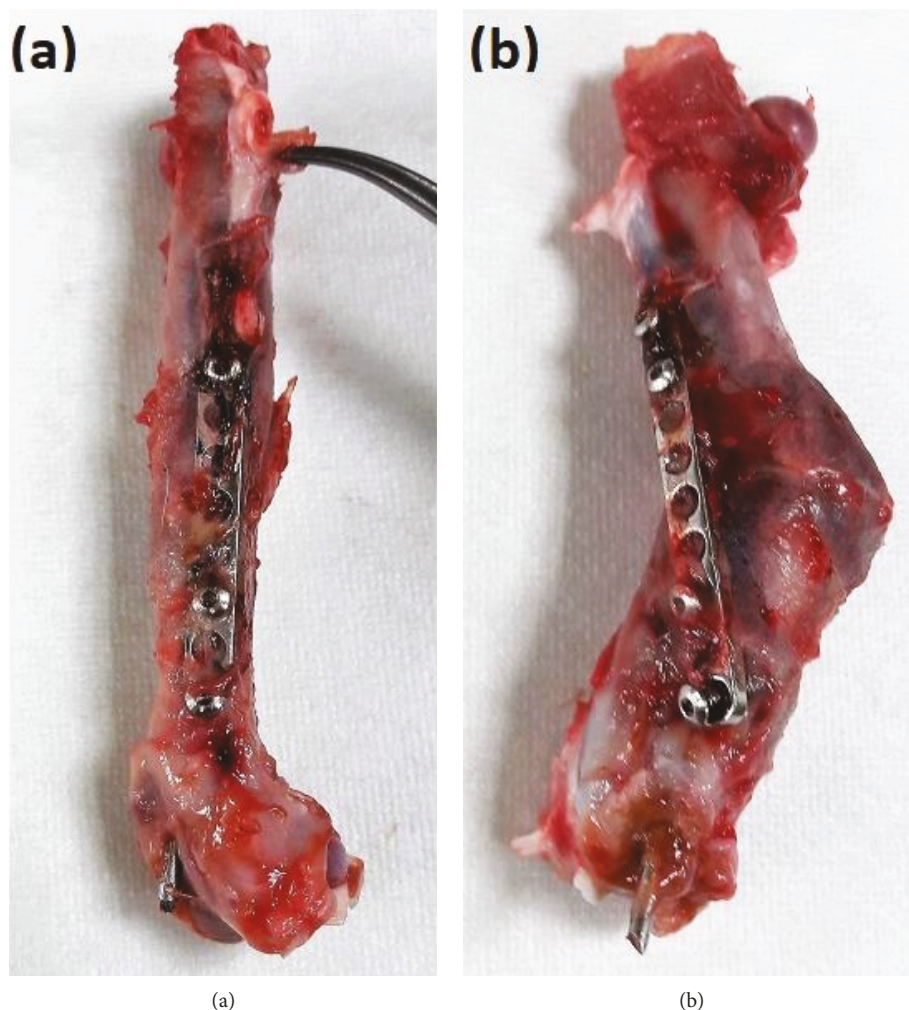


FIGURE 4: Representative images of the examined femoral defects after the rabbit euthanization. (a) Representative images of the BG group femur, showing a continuous femoral cortex with good union rate without deformity. (b) Representative images of a malunited femur obtained from an animal included in the BG-f group, with the loss of the fixation of applied fixators.

PMMA spacer is a crucial step in this procedure, as it prevents the fibrous tissues from invading the bone defect (mechanical role) and induces the growth of surrounding membrane (biological role) that envelops bone grafts and stimulates bone healing mediated by osteoinductive growth factors [29–31]. However, the PMMA cement spacer needs to be surgically removed, so that the bone graft can be implanted within the “envelop” generated by the PMMA spacer. The PLGA nanofibers examined in this study exhibited a similar ability to induce the development of bioactive membranes, as shown by histologic and IHC analyses. Additionally, the bone healing process was shown to proceed simultaneously with the degradation of the PLGA nanofibers in the BG group, indicating that these grafts were securely fixed inside the PLGA nanofiber layer. With the formation of the induced membrane and degradation of the PLGA nanofibers, new bone formation was stimulated, suggesting that the PLGA nanofibers and this membrane may play a role as a bone graft reservoir. By using the biodegradable nanofibers, the original two-

stage Masquelet procedure can be reduced to a single step, decreasing the time, cost, and patient discomfort associated with the treatment, in addition to minimizing the risk of surgical site infection.

Our study has several limitations. First, the rabbits used in the study were all euthanized at 6 weeks, and this time point was selected based on the timing of the standard Masquelet procedure, as in previous studies [12–16]. To the best knowledge of the authors, this research was the pioneer in using biodegradable material to induce a bioactive membrane. Therefore, the actual time necessary to induce membrane formation was unknown. However, we successfully induced bioactive membrane formation, which the results of our analyses confirmed. Furthermore, due to the loss of the fixation of one femur in the BG group, its shape was shown to be deformed, with shortening of the bone. However, the results obtained from both groups demonstrated that the preservation of bone grafts is crucial for bone healing. Finally, we did not quantify the obtained micro-CT results, failing to determine the quantitative difference

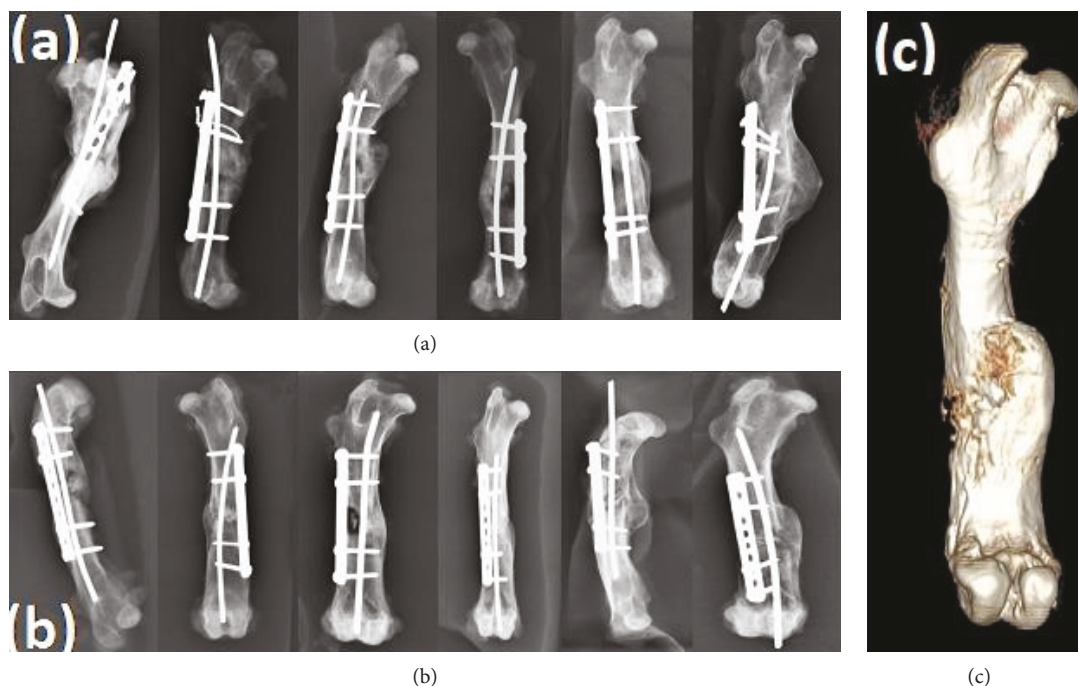


FIGURE 5: X-ray and microcomputed tomography (CT) evaluations of the treated femoral defects. (a) Representative X-ray images of the treated femoral defects in the BG-f group. (b) Representative X-ray images of the treated femoral defects in the BG group. (c) Representative micro-CT images of the treated femoral defects in the BG group.

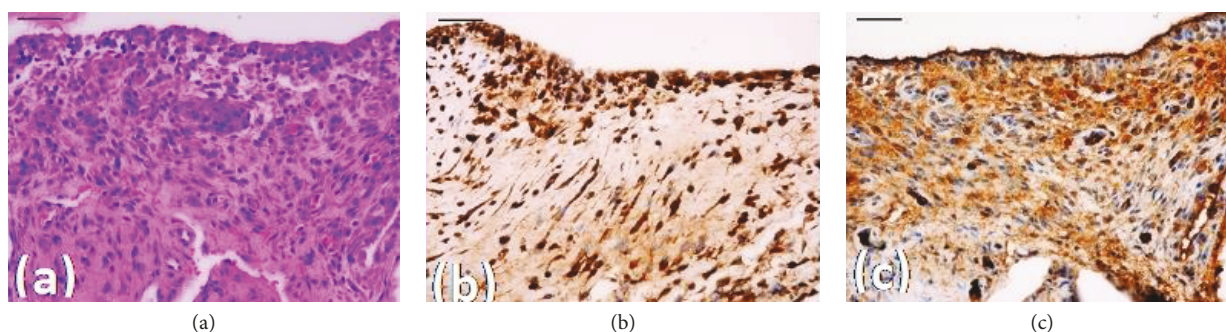


FIGURE 6: Histologic and immunohistochemical examination of the femoral samples. (a) Capsular membrane stained with hematoxylin and eosin. (b) BMP2 and (c) VEGF expression in the femoral samples. Scale bars, 50 μm .

between the analyzed groups. However, the union rates can be determined from the photographs and X-ray images. In future, these differences should be quantified.

5. Conclusion

In conclusion, in this study, we successfully used the PLGA nanofibers as a biodegradable material in the Masquelet technique, which were shown to induce the generation of bioactive membranes, envelope bone grafts, and enhance bone union. We demonstrated additionally that this material can replace the PMMA in the treatment of large bone defects, and it does not need to be removed. Further studies should focus on the duration of postoperative induction of membrane formation and the use of

different biodegradable materials with better performance than the PLGA nanofibers.

Data Availability

The data used to support the findings of this study are available from the corresponding author upon request.

Disclosure

YH Yu and RC Wu are co-first authors of this paper.

Conflicts of Interest

The authors declare that there is no conflict of interest.

Authors' Contributions

Conceptualization was handled by Y.-H.Y. and S.-J.L., funding acquisition was handled by S.-J.L., the investigation was handled by Y.-H.Y. and C.-K.C., the manuscript was written by Y.-H.Y. and R.-C.W., review and editing of the written manuscript was handled by D.L., and supervision of the research was handled by S.-J.L. YH Yu and RC Wu contributed equally to this work.

Acknowledgments

The financial supports of the Ministry of Science and Technology, Taiwan (Contract No. 107-2221-E-182-017) and Chang Gung Memorial Hospital (Contract No. CMRPD2G0252) for this research are gratefully acknowledged. An earlier version of the manuscript is submitted as a preprint: <https://www.preprints.org/manuscript/201806.0047/v1>.

References

- [1] M. E. Hake, J. K. Oh, J. W. Kim et al., "Difficulties and challenges to diagnose and treat posttraumatic long bone osteomyelitis," *European Journal of Orthopaedic Surgery and Traumatology*, vol. 25, no. 1, pp. 1–3, 2015.
- [2] A. Nauth, M. D. McKee, T. A. Einhorn, J. T. Watson, R. Li, and E. H. Schemitsch, "Managing bone defects," *Journal of Orthopaedic Trauma*, vol. 25, no. 8, pp. 462–466, 2011.
- [3] G. I. Taylor, G. D. Miller, and F. J. Ham, "The free vascularized bone graft. A clinical extension of microvascular techniques," *Plastic and Reconstructive Surgery*, vol. 55, no. 5, pp. 533–544, 1975.
- [4] C. S. Molina, D. J. Stinner, and W. T. Obrebsky, "Treatment of traumatic segmental long-bone defects. A critical analysis review," *JBJS Reviews*, vol. 2, no. 4, p. 1, 2014.
- [5] T. R. Madhusudhan, B. Ramesh, K. Manjunath, H. M. Shah, D. C. Sundaresh, and N. Krishnappa, "Outcomes of Ilizarov ring fixation in recalcitrant infected tibial non-unions—a prospective study," *Journal of Trauma Management & Outcomes*, vol. 2, no. 1, p. 6, 2008.
- [6] C. W. Oh, T. Apivatthakakul, J. K. Oh et al., "Bone transport with an external fixator and a locking plate for segmental tibial defects," *The Bone & Joint Journal*, vol. 95-B, no. 12, pp. 1667–1672, 2013.
- [7] B. Demiralp, T. Ege, O. Kose, Y. Yurttas, and M. Basbozkurt, "Reconstruction of intercalary bone defects following bone tumor resection with segmental bone transport using an Ilizarov circular external fixator," *Journal of Orthopaedic Science*, vol. 19, no. 6, pp. 1004–1011, 2014.
- [8] M. Chaddha, D. Gulati, A. P. Singh, A. P. Singh, and L. Maini, "Management of massive posttraumatic bone defects in the lower limb with the Ilizarov technique," *Acta Orthopaedica Belgica*, vol. 76, no. 6, pp. 811–820, 2010.
- [9] P. V. Giannoudis, "Treatment of bone defects: bone transport or the induced membrane technique?," *Injury*, vol. 47, no. 2, pp. 291–292, 2016.
- [10] A. C. Masquelet, F. Fitoussi, T. Begue, and G. P. Muller, "Reconstruction of the long bones by the induced membrane and spongy autograft," *Annales de Chirurgie Plastique et Esthétique*, vol. 45, no. 3, pp. 346–353, 2000.
- [11] P. Pelissier, D. Martin, J. Baudet, S. Lepreux, and A. C. Masquelet, "Behaviour of cancellous bone graft placed in induced membranes," *British Journal of Plastic Surgery*, vol. 55, no. 7, pp. 596–598, 2002.
- [12] C. Karger, T. Kishi, L. Schneider, F. Fitoussi, A. C. Masquelet, and For French Society of Orthopaedic Surgery and Traumatology (SoFCOT), "Treatment of posttraumatic bone defects by the induced membrane technique," *Orthopaedics & Traumatology: Surgery & Research*, vol. 98, no. 1, pp. 97–102, 2012.
- [13] B. C. Taylor, J. Hancock, R. Zitzke, and J. Castaneda, "Treatment of bone loss with the induced membrane technique: techniques and outcomes," *Journal of Orthopaedic Trauma*, vol. 29, no. 12, pp. 554–557, 2015.
- [14] U. K. Olesen, H. Eckardt, P. Bosemark, A. W. Paulsen, B. Dahl, and A. Hede, "The Masquelet technique of induced membrane for healing of bone defects. A review of 8 cases," *Injury*, vol. 46, Supplement 8, pp. S44–S47, 2015.
- [15] A. O. Scholz, S. Gehrmann, M. Glombitza et al., "Reconstruction of septic diaphyseal bone defects with the induced membrane technique," *Injury*, vol. 46, Supplement 4, pp. S121–S124, 2015.
- [16] M. Ronga, S. Ferraro, A. Fagetti, M. Cherubino, L. Valdatta, and P. Cherubino, "Masquelet technique for the treatment of a severe acute tibial bone loss," *Injury*, vol. 45, Supplement 6, pp. S111–S115, 2014.
- [17] R. Morris, M. Hossain, A. Evans, and I. Pallister, "Induced membrane technique for treating tibial defects gives mixed results," *The Bone & Joint Journal*, vol. 99-B, no. 5, pp. 680–685, 2017.
- [18] W. Peng, W. Zheng, K. Shi, W. Wang, Y. Shao, and D. Zhang, "An in vivo evaluation of PLLA/PLLA-gHA nano-composite for internal fixation of mandibular bone fractures," *Biomedical Materials*, vol. 10, no. 6, article 065007, 2015.
- [19] H. K. Uthoff, P. Poitras, and D. S. Backman, "Internal plate fixation of fractures: short history and recent developments," *Journal of Orthopaedic Science*, vol. 11, no. 2, pp. 118–126, 2006.
- [20] T. Suto, H. Obata, M. Tobe et al., "Long-term effect of epidural injection with sustained-release lidocaine particles in a rat model of postoperative pain," *British Journal of Anaesthesia*, vol. 109, no. 6, pp. 957–967, 2012.
- [21] Y. H. Yu, Y. H. Hsu, Y. C. Chou et al., "Sustained relief of pain from osteosynthesis surgery of rib fracture by using biodegradable lidocaine-eluting nanofibrous membranes," *Nanomedicine: Nanotechnology, Biology and Medicine*, vol. 12, no. 7, pp. 1785–1793, 2016.
- [22] J. Ferguson, M. Diefenbeck, and M. McNally, "Ceramic biocomposites as biodegradable antibiotic carriers in the treatment of bone infections," *Journal of Bone and Joint Infection*, vol. 2, no. 1, pp. 38–51, 2017.
- [23] Y. C. Chou, D. Lee, T. M. Chang et al., "Development of a three-dimensional (3D) printed biodegradable cage to convert morselized corticocancellous bone chips into a structured cortical bone graft," *International Journal of Molecular Sciences*, vol. 17, no. 4, p. 595, 2016.
- [24] S. Casagrande, R. Tiribuzi, E. Casseti et al., "Biodegradable composite porous poly(dl-lactide-co-glycolide) scaffold supports mesenchymal stem cell differentiation and calcium phosphate deposition," *Artificial Cells, Nanomedicine, and Biotechnology*, pp. 1–11, 2017.

- [25] S. G. Kumbar, S. P. Nukavarapu, R. James, L. S. Nair, and C. T. Laurencin, "Electrospun poly(lactic acid-co-glycolic acid) scaffolds for skin tissue engineering," *Biomaterials*, vol. 29, no. 30, pp. 4100–4107, 2008.
- [26] A. C. Masquelet, "Induced membrane technique: pearls and pitfalls," *Journal of Orthopaedic Trauma*, vol. 31, Supplement 5, pp. S36–S38, 2017.
- [27] P. V. Giannoudis, O. Faour, T. Goff, N. Kanakaris, and R. Dimitriou, "Masquelet technique for the treatment of bone defects: tips-tricks and future directions," *Injury*, vol. 42, no. 6, pp. 591–598, 2011.
- [28] C. Mauffrey, M. E. Hake, V. Chadayammuri, and A. C. Masquelet, "Reconstruction of long bone infections using the induced membrane technique: tips and tricks," *Journal of Orthopaedic Trauma*, vol. 30, no. 6, pp. e188–e193, 2016.
- [29] X. Wang, F. Wei, F. Luo, K. Huang, and Z. Xie, "Induction of granulation tissue for the secretion of growth factors and the promotion of bone defect repair," *Journal of Orthopaedic Surgery and Research*, vol. 10, no. 1, p. 147, 2015.
- [30] C. Christou, R. A. Oliver, Y. Yu, and W. R. Walsh, "The Masquelet technique for membrane induction and the healing of ovine critical sized segmental defects," *PLoS One*, vol. 9, no. 12, article e114122, 2014.
- [31] C. H. Ma, Y. C. Chiu, K. L. Tsai, Y. K. Tu, C. Y. Yen, and C. H. Wu, "Masquelet technique with external locking plate for recalcitrant distal tibial nonunion," *Injury*, vol. 48, no. 12, pp. 2847–2852, 2017.



Hindawi
Submit your manuscripts at
www.hindawi.com

